Available online at www.sciencedirect.com
ScienceDirect
Catalysis Today 130 (2008) 199–205
CATALYSIS TODAY
www.elsevier.com/locate/cattod

Kinetics of thiophene reactive adsorption on Ni/SiO_2 and Ni/ZnO

Igor Bezverkhyy *, Andrey Ryzhikov, Geoffroy Gadacz, Jean-Pierre Bellat

Institut Carnot de Bourgogne, UMR 5209 CNRS-Université de Bourgogne, 9 av. A. Savary BP 47870, 21078 Dijon Cedex, France

Available online 23 July 2007

Abstract

Kinetics of thiophene reactive adsorption on Ni/SiO_2 and Ni/ZnO was studied by thermal gravimetric analysis at 280–360 °C under 5–40 mbar of thiophene in H_2. In the case of Ni/SiO_2 the interaction proceeds in two steps: a rapid surface reaction is followed by a slower bulk transformation into Ni_3S_2. Maximum Ni conversion depends on reaction conditions and observed conversion profiles can be described by an exponential equation corresponding to a reaction of first order relatively to both sulfidable Ni amount and thiophene. The interaction between Ni/ZnO and thiophene proceeds in a rather different manner. A rapid increase of weight, similar to the first stage observed on Ni/SiO_2, is not followed by bulk Ni sulfidation, but instead by a nucleation-controlled ZnO surface transformation. After formation of the surface ZnS layer, a complete particles sulfidation occurs with kinetics being strongly dependent on the reaction conditions possibly due to comparable rates of different reaction steps.

Keywords: Reactive adsorption; Desulfurization; Thiophene adsorption; Supported Ni

1. Introduction

Removal of sulfur from refinery streams remains one of the most challenging tasks in petroleum industry [1,2]. Although the appearance of new, more active catalyst formulations, enables hydrodesulfurization (HDS) process to produce fuels with a <10–50 ppm S grade, this approach shows a disadvantage of unnecessary hydrogenation of hydrocarbons while removing sulfur species, resulting in an excessive hydrogen cost imposed for refineries. For this reason development of alternatives to classic HDS attracted much interest in recent years [3]. While classical HDS continues to be the only industrially viable technology for diesel hydrotreatment, a panoply of new methods has appeared for gasoline ultra-deep desulfurization with Prime G+ and SCANfining being today the technologies of choice [4]. Although these novel catalytic approaches allow to satisfy the stringent norms on sulfur content (<10–50 ppm S), a loss of octane number is still an intrinsic issue of catalytic hydrodesulfurization processes. That is why development of other methods, based on adsorption or oxidation of sulfur species, continues to attract considerable attention.

One of such novel methods, reactive adsorption, has been implemented in *S-Zorb* desulfurization technology used on industrial scale [5]. In this approach sulfur-containing molecules *react* with a solid adsorbent in the presence of hydrogen [6]. During the reaction the active phase of the adsorbent, consisting of metallic particles supported on ZnO, is transformed into a mixture of sulfides. After complete transformation (saturation) the adsorbent is regenerated in a two-stage process: sulfides are firstly calcined to obtain oxides which are than treated in H_2 in order to reduce the supported metal. The method was demonstrated to possess some valuable features like low hydrogen consumption and absence of side hydrogenation reactions provoking decrease in octane number [7]. Despite these advantages, very little is known about the mechanism of reactive adsorption. It was supposed that ZnO acts as an acceptor for sulfur produced from sulfur-containing molecules on Ni particles which were suggested to be "continuously regenerated" during reaction [6]. Babich and Moulijn proposed a reaction scheme in which thiophene is decomposed on metal surface with following hydrogenation of NiS site and transfer of H_2S to ZnO [1]. However, the key points of the proposed mechanism of reactive adsorption have not yet been understood. It is not clear if sulfur-containing molecules are decomposed by HDS reaction on metallic particles or a novel mechanism operates in this system. Also, we do not know if the reaction is limited by decomposition of sulfur-containing species or by ZnO sulfidation.

* Corresponding author. Tel.: +33 380 39 61 84; fax: +33 380 39 61 32.
E-mail address: igor.bezverkhyy@u-bourgogne.fr (I. Bezverkhyy).

0920-5861/$ – see front matter © 2007 Elsevier B.V. All rights reserved.
doi:10.1016/j.cattod.2007.06.038

In the present work, we studied reactive adsorption of thiophene in gas phase on a model system Ni/SiO_2 and on an industrially relevant adsorbent Ni/ZnO. Thermal gravimetric analysis was used to characterize the reaction kinetics under varying temperature and thiophene partial pressure. Based on these experimental data, we propose a kinetic description of the interaction and suggest some features of the reaction mechanism for two types of materials.

2. Experimental

$Ni(NO_3)_2{\cdot}6H_2O$ of reactive grade, which was used as Ni precursor, was purchased from Aldrich. Ni/SiO_2 was prepared by homogeneous deposition–precipitation on Aerosil 200 (Degussa, $S_{BET} = 223\ m^2/g$). 4.942 g (0.017 mol) of $Ni(NO_3)_2{\cdot}6H_2O$ were dissolved in 190 mL of water and 4 g of Aerosil were suspended in the solution. pH of the mixture was adjusted to 3.5 with HNO_3 and 5.00 g (0.083 mol) of urea was added. The obtained suspension was heated at 90 °C under vigorous stirring for 30 h, the time necessary to obtain a colorless solution. The solid was filtered, thoroughly washed with water and dried in oven overnight at 100 °C. After drying the sample was directly reduced in hydrogen. Firstly, it was heated at 1 °C/min to 230 °C and reduced at this temperature for 1 h. Then the temperature was raised (at 2 °C/min) to 600 °C and maintained for 10 h (such a treatment allows to reduce Ni completely without silicate formation [8]). After reduction the samples were cooled down and passivated in order to avoid a strongly exothermic Ni oxidation upon a direct contact of between reduced Ni and air. The typical procedure described in literature [9] was used. Firstly the sample was purged with a flow consisting of 1 mL/min of air and 100 mL/min of N_2 and then air content was gradually raised before exposure to air.

Ni/ZnO samples were synthesized by co-precipitation of $Zn(NO_3)_2{\cdot}6H_2O$ (reactive grade, Aldrich) and $Ni(NO_3)_2{\cdot}6H_2O$ by sodium carbonate. 6.576 g (0.0221 mol) $Zn(NO_3)_2{\cdot}6H_2O$ and 0.778 g (0.0027 mol) $Ni(NO_3)_2{\cdot}6H_2O$ were dissolved in 127 mL of water to obtain 0.2 M solution. Taken quantities correspond to 10 wt% of NiO in NiO/ZnO sample. Co-precipitation was done by dropwise addition of equimolar quantity of 0.5 M solution of Na_2CO_3 under vigorous stirring. Obtained suspension was stirred during 12 h, and then the solid was filtered, thoroughly washed with water and dried in oven overnight at 100 °C. After drying the sample was annealed in air at 400 °C for 4 h (heating rate, 2 °C/min). This was followed by a reduction in hydrogen flow at 400 °C for 5 h. After reduction the samples were cooled down and passivated in the same way as Ni/SiO_2 samples.

X-ray diffraction patterns of the samples were recorded using an INEL CPS120 semicircle counter using Cu Kα monochromatic radiation. Transmission electron microscopy micrographs were obtained on a JEOL JEM 2100 instrument. Ni particles average size in Ni/SiO_2 was obtained from measuring 350–400 particles on different sample areas. The given value is the average weighted by volume:

$$\bar{d} = \frac{\sum_i n_i d_i^4}{\sum_i n_i d_i^3}$$

BET surface areas were measured on a BEL Mini apparatus by N_2 adsorption at 77 K. Chemical analysis of the samples was done by Central Analysis Service (SCA) of the French National Centre for Scientific Research (CNRS).

For thermal gravimetric study of the reaction kinetics a home-made setup was used. The sample was suspended in a silica tube in which a down-up gas flow passed. The sample weight was recorded using a SETARAM B85 balance head which was continuously purged with nitrogen. Before the reaction the solids were reduced in H_2 flow (150 mL/min) during 3 h at 600 °C (Ni/SiO_2) or at 360 °C during 6 h (Ni/ZnO). These conditions are sufficient to reduce completely Ni particles as it follows from TGA (data not shown). After the sample has been reduced, a thiophene/H_2 reaction mixture was brought into the tube. Preliminary experiments were performed in order to determine the operating conditions which would exclude any influence of mass transfer in gas phase and between the powder particles. It was found that a gas flow greater than 130 mL/min should be used and the mass of the sample should not exceed 30 mg. Therefore, the hydrogen flow of 150 mL/min and samples of 20 mg were used systematically throughout this study. The conversion was calculated in the following way:

$$X(t) = \frac{W(t) - W_0}{W(\mathrm{S})_{\max}} \quad \text{for} \quad Ni/SiO_2$$

$$X(t) = \frac{W(t) - W_0}{\Delta W_{\max}} \quad \text{for} \quad Ni/ZnO$$

where $W(t)$ is the sample weight at instant t, W_0 the sample weight after reduction, $W(\mathrm{S})_{\max}$ the maximum amount of sulfur which can react with Ni, and $\Delta W_{\max}$ is the maximum weight change for Ni/ZnO sample. In all cases Ni was supposed to be transformed into Ni_3S_2 and ZnO into ZnS.

3. Results and discussion

3.1. Solids characterization

Composition and textural properties of the solids used in the work are given in Table 1. For Ni/SiO_2 samples we used a nonporous Aerosil silica as support in order to exclude any eventual intrusion of pore diffusion in the overall interaction kinetics. Supported Ni particles have small size and narrow size distribution (3–6 nm) which are typical features of supported material prepared by homogeneous deposition–precipitation [9].

XRD pattern of Ni/ZnO shows presence of NiO despite passivation procedure. To obtain the size of Ni particles (Table 1), the size of NiO was therefore corrected using the ratio

Table 1
Composition and textural properties of the samples used in the work

Sample	S_{BET} (m^2/g)	Ni (wt%)	d_{Ni} (nm)	d_{ZnO} (nm)
Ni/SiO_2	244	17.3	5.2 (TEM)	
Ni/ZnO	32	6.1	5.3[a] (XRD)	14 (XRD)

[a] Calculated from the size of NiO particles using the ratio of molar volumes of Ni and NiO.

of molar volumes of Ni and NiO. In the case of Ni/ZnO the contrast in TEM is too weak to determine with precision Ni particle size. Nevertheless, we could identify some domains as being NiO particles using EDX analysis. Their size, *ca.* 6 nm, is close to the value estimated from XRD. TEM shows also that ZnO particles are of two types: 20–30 and ∼10 nm. BET surface area of Ni/ZnO sample is lower than the surface estimated from average crystallite size determined by XRD ($S = 6/(\rho d)$, ∼80 m^2/g). This difference can be due to partial crystallite agglomeration.

3.2. Interaction between thiophene and Ni/SiO_2

Conversion profiles for silica supported Ni, measured at different temperatures, are given in Fig. 1a. Two different regions can be distinguished in all curves. The first one corresponds to a fast weight change occurring immediately after contact with thiophene vapor. It seems natural to suppose that this increase is due to formation of surface sulfide on reduced Ni particles. It is well known that such phase, referred to as ''surface'' or ''two-dimensional'', forms rapidly on metal surface upon the contact with sulfur-containing species [10,11]. In our case formation of this phase is supported by the fact that the fraction of Ni consumed during the first stage (*ca.* 18%) is close to a number of exposed Ni surface atoms (metal dispersion) usually reported for samples prepared by deposition–precipitation [9].

The first rapid step is followed by a much slower weight increase corresponding to sulfidation of the bulk of Ni particles and leading to Ni_3S_2 as shown by ex situ XRD analysis after reaction. Surprisingly, the reaction is not complete and the maximum conversion depends on temperature and thiophene partial pressure (Figs. 1a and 2a). The reason why Ni is not completely sulfided despite a significant thiophene partial pressure is not clear so far. It can be supposed that the reaction is size-dependent and only particles below a certain critical size (whose value depends on conditions) are sulfided. Such a phenomenon was suggested for Co oxidation in Fischer–Tropsch reaction on Co/SiO_2 [12] and was experimentally observed in oxidation of supported Pd clusters [13]. Another possibility is the reverse reaction of hydrogen with Ni_3S_2. That is, partial conversion can be due to existence of the equilibrium: $3/2Ni + H_2S \leftrightarrow 1/2Ni_3S_2 + H_2$. According to thermodynamic data [10], at 360 °C equilibrium pressure of H_2S is about

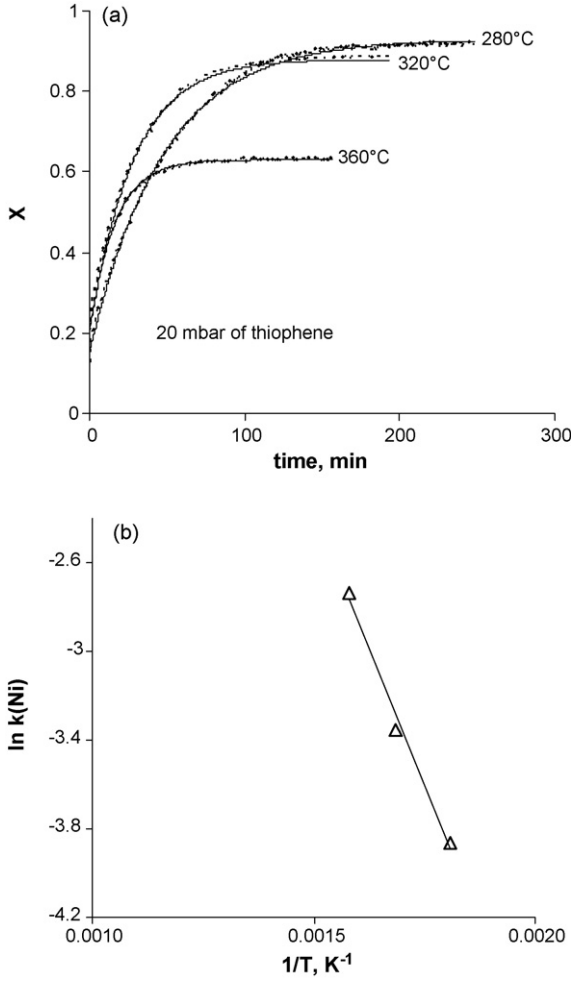

Fig. 1. Effect of temperature on the conversion profiles of Ni/SiO_2 in thiophene/H_2 flow (broken line, experimental points; solid line, fit with Eq. (2)) (a) and corresponding Arrhenius plot of the apparent first order rate constant *k*(Ni) (b).

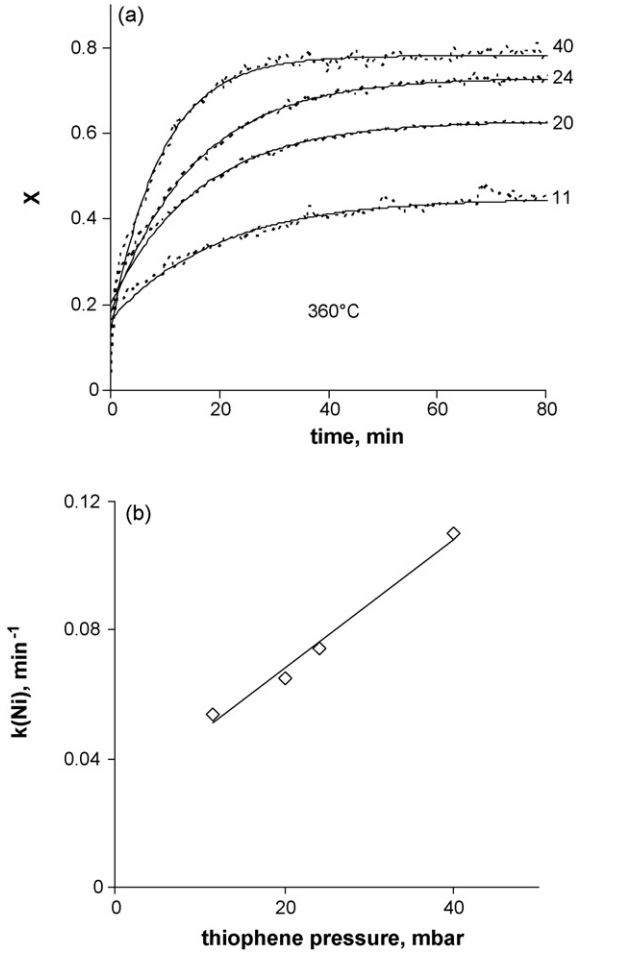

Fig. 2. Effect of thiophene partial pressure (in mbar) on the conversion profiles of Ni/SiO_2 in thiophene/H_2 flow (broken line, experimental points; solid line, fit with Eq. (2)) (a) and variation of the apparent first order rate constant *k*(Ni) with thiophene pressure (b).

0.02 mbar. Hence, this equilibrium could be realized only if thiophene conversion to H_2S is very low. Studies are under way to verify this assumption.

To fit the obtained conversion profiles we tried firstly to apply the equations derived from the shrinking-core model [14]. We noticed however that in the case of spherical symmetry these equations allow to fit the beginning of the curve, but they fail to represent correctly the saturation at conversion lower than unity. Other relationships, showing an asymptotic behavior, were tried and it was found that an exponential function permits to fit correctly the experimental data. The corresponding equation can be obtained if we suppose a first order reaction relatively to Ni:

$$\frac{dX}{dt} = k(\mathrm{Ni})(X_m - X) \quad (1)$$

where X is the fraction of converted Ni at instant t, X_m the maximum Ni conversion, k(Ni) is the apparent first order rate constant. Integrating this equation with $X = X_0$ at $t = 0$, we obtain

$$X = X_0 e^{-k(\mathrm{Ni})t} + X_m(1 - e^{-k(\mathrm{Ni})t}) \quad (2)$$

or

$$\ln\frac{X_m - X}{X_m - X_0} = -k(\mathrm{Ni})t \quad (3)$$

where X_0 is the conversion attained in the first step.

Using two experimental parameters X_m and X_0 we can calculate in this way the apparent first order rate constant k(Ni) (Table 2). The dependence of ln(k(Ni)) on inverse temperature gives an Arrhenius type plot from which the activation energy of the reaction can be calculated (Fig. 1b). The value obtained (40 kJ/mol) clearly shows that the reaction is not controlled by ionic diffusion, for which much higher values (150–200 kJ/mol) are generally observed [15]. Variation of thiophene partial pressure has a double effect on the conversion (Fig. 2): the maximum value (X_m) augments with pressure and in the same time the rate constant k(Ni) increases linearly (Fig. 2b). The latter fact shows that reaction is also of first order relatively to thiophene and the reaction rate can be written in the following way:

$$r = \frac{dX}{dt} = k(\mathrm{Ni})[\mathrm{Ni}] = k[\mathrm{thiophene}][\mathrm{Ni}]$$

where k is the second order rate constant, [thiophene] thiophene concentration, and [Ni] is the sulfidable Ni concentration.

The behavior of supported Ni nanoparticles in the reaction with thiophene is rather different from that of bulk metal samples in the sulfur-containing atmosphere. In fact, for macroscopic metals diffusion of cations is generally a rate-limiting step [16]. In our case the value of activation energy as well as a linear pressure dependence of the rate constant excludes such a possibility. Moreover, the validity of the homogeneous-like kinetic description points out that classical approach, distinguishing reaction and diffusion, may be impertinent in the case of nanoparticles. This is due to an extremely low product film thickness in such systems. Indeed,

Table 2
Rate constants for the reaction between thiophene and Ni/SiO_2 under different reaction conditions (calculated from Eq. (3))

Thiophene pressure (mbar)	t (°C)	k(Ni) (min^{-1})
20	280	0.021
20	320	0.035
20	360	0.065
11	360	0.054
24	360	0.074
40	360	0.11

for spherical shrinking particle of constant size the transformation degree is given by

$$X = 1 - \left(\frac{r}{R}\right)^3 \quad (4)$$

where R is the initial particle size and r is the size of unreacted core.

The thickness of the product layer in this case will be:

$$\Delta r = R - r = R - R(1 - X)^{1/3} = R(1 - (1 - X)^{1/3}) \quad (5)$$

For R = 25 Å at X = 0.5 the thickness of the product layer is only 5.2 Å, which is comparable to Ni_3S_2 cell parameter (4 Å). Two interfaces, metal–sulfide and sulfide–gas, are therefore separated in our case only by few atomic layers. It is doubtful that in such situation we can really distinguish chemical steps (transfer through interfaces) from diffusion.

3.3. Reactive adsorption of thiophene on Ni/ZnO

For Ni/ZnO reacting with thiophene the weight change follows a complex pattern in which at least three different domains can be distinguished (Fig. 3). At the beginning the conversion increases rapidly up to *ca.* 0.07–0.1 and the rate of this step is not much influenced by temperature or thiophene pressure. This initial weight increase is followed by a S-shaped domain up to $X \sim 0.25$ and then the reaction rate decreases giving a straight line at 360 °C and 20 mbar. Under other reaction conditions this part of the curve deviates from straight line becoming concave (Fig. 3). In contrast to Ni/SiO_2, maximum conversion of Ni/ZnO does not depend on conditions and it is close to unity.

The rapid weight increase of Ni/ZnO at the beginning of reaction can have the same origin as in the case of Ni/SiO_2. A layer of chemisorbed sulfur on Ni surface forms rapidly after the contact with thiophene/H_2 mixture. The S-shaped part of the curve is characteristic of a process controlled by nucleation and growth of new phase [17]. To describe this part we tried the Avrami–Erofeev equation:

$$X = 1 - e^{-(k_{AE}(\mathrm{Ni})(t - t_i))^n} \quad (6)$$

where k_{AE}(Ni) is the rate constant, t_i the induction time and n depends on the dimensionality of the nuclei and on the nature of the nucleation reaction [18]. It was found that this equation is applicable in our case from time t_i and gives the best fit of the data if n = 1.5–2. The precise value of n is difficult to extract

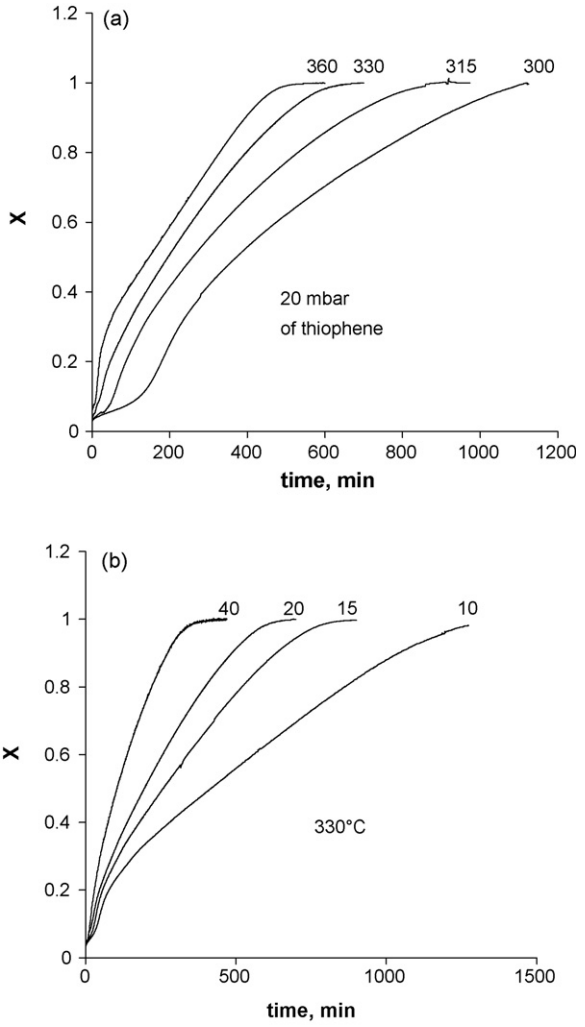

Fig. 3. Conversion profiles of Ni/ZnO at different temperatures under 20 mbar of thiophene in H_2 (a), and under different thiophene pressures (in mbar) at 330 °C (b).

from the experimental data as only a part of the curve can be fitted and also because n value is strongly influenced by the choice of t_i. Taking into account that the described domain is not a complete reaction (from $X = 0$ to $X = 1$) but a reaction step between X_1 and X_2 the following equation was used to fit the region $X = 0.07$–0.2:

$$X = X_1 + (X_2 - X_1)(1 - e^{-(k_{AE}(Ni)(t-t_i))^n}) \quad (7)$$

or in a linear form:

$$\ln\left(1 - \frac{X - X_1}{X_2 - X_1}\right) = -(k_{AE}(Ni)(t - t_i))^n \quad (8)$$

The obtained values of k_{AE}(Ni) are given in Table 3 and quality of the fit for $n = 1.5$ is illustrated in Figs. 4a and 5a. Tracing ln(k_{AE}(Ni)) as a function of $1/T$ gives a straight line (Fig. 4b) from which the activation energy of 94 kJ/mol was calculated. Also, the Avrami–Erofeev rate constant depends linearly on thiophene partial pressure (Fig. 5b).

Some features of the reaction mechanism in the domain $X \sim 0.07$–0.25 can be drawn from this data. The shape of the

Table 3
Rate constant from Avrami–Erofeev equation (k_{AE}(Ni)) and average reaction rates ($X = 0.4$–0.6) for Ni/ZnO under different reaction conditions

Thiophene pressure (mbar)	t (°C)	k_{AE}(Ni) (min^{-1})	$\bar{v}$ (10^{-7} mol S/g s)
20	300	0.016	2.2
20	315	0.031	2.7
20	330	0.048	3.5
20	360	0.105	3.6
10	330	0.034	1.5
15	330	0.042	2.6
40	330	0.074	6.6

curve is characteristic of a nucleation-controlled transformation of the surface layer giving a continuous reaction interface. The calculated value of $n = 1.5$–2 in the Avrami–Erofeev equation is consistent with a two-dimensional growth of the nuclei whose formation rate decreases as reaction proceeds [18]. In our case the induction time corresponds to formation of ZnS nuclei which grow on the surface of ZnO particles covering them progressively with a continuous ZnS layer.

The shape of the curves for $X > 0.25$, corresponding to bulk ZnO sulfidation, changes noticeably when temperature is varied

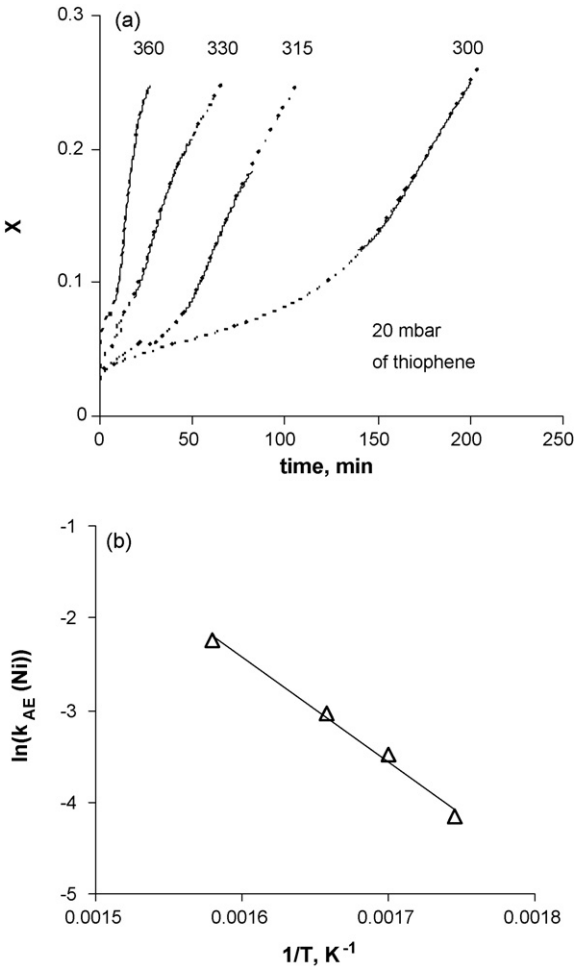

Fig. 4. S-shaped domain of the conversion profiles of Ni/ZnO at different temperatures (broken line, experimental data; solid line, fit with Eq. (7)) (a), Arrhenius plot of the constants k_{AE} (Ni)(b).

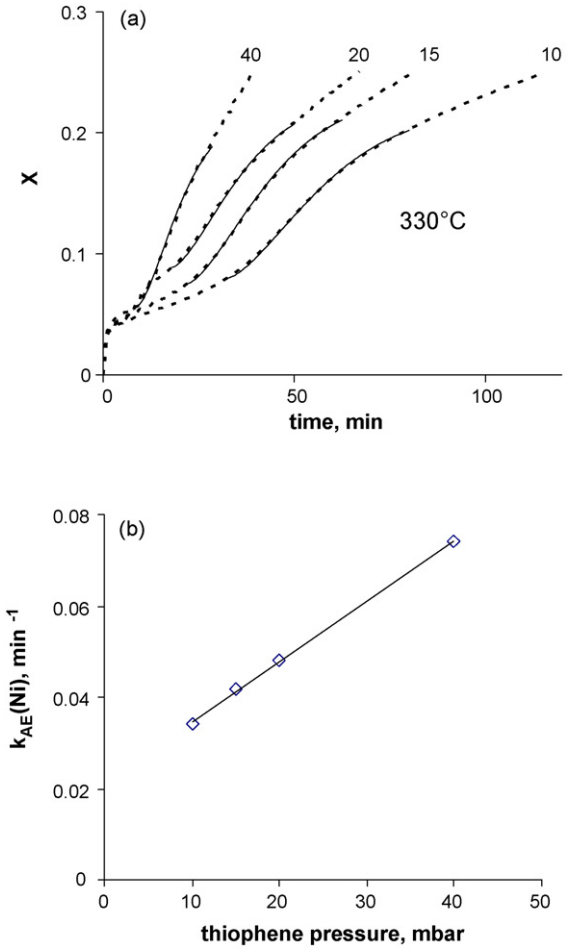

Fig. 5. S-shaped domains of the conversion profiles of Ni/ZnO under different thiophene pressures (broken line, experimental data; solid line, fit with Eq. (7)) (a), pressure dependence of the rate constants k_{AE}(Ni) (b).

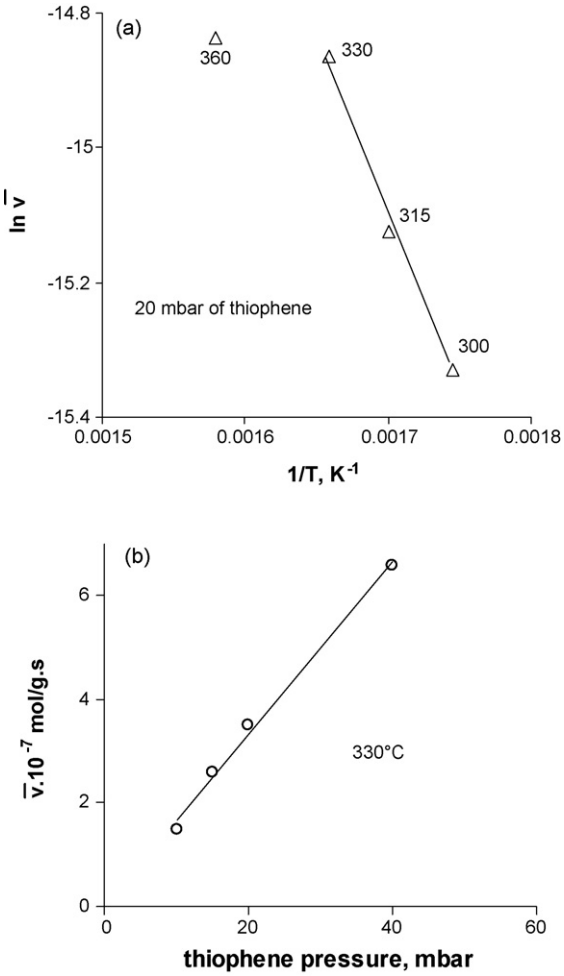

Fig. 6. Arrhenius plot for Ni/ZnO of the average rate for conversion between 0.4 and 0.6 (a), pressure dependence of the average rate for conversion between 0.4 and 0.6 (b).

between 300 and 360 °C (Fig. 3a). It means that in this temperature domain the reaction is controlled by two different processes with similar rates. The contribution of each process can vary with temperature (due to a difference in their activation energies) which leads to a smooth variation of the shape of conversion profiles. In such a case the time dependence of X cannot be described by a simple analytic expression [14]. However, the obtained curves are close to straight lines and we tried to estimate the activation energy using average rate values ($\bar{v} = \Delta X/\Delta t$) calculated between $X = 0.4$ and $X = 0.6$ (Table 3). The value obtained (44 kJ/mol) is lower than for the surface sulfidation. Also we note that in the corresponding Arrhenius type plot $\ln(\bar{v})$–$1/T$ (Fig. 6a) the point 360 °C stands apart from the straight line pointing out to the change of the rate determining process.

It would be natural to suppose that the rate determining step for bulk ZnO sulfidation ($X > 0.25$) is diffusion through surface ZnS layer. However, the analysis of the curves shape does not confirm this assumption for high temperatures. Indeed, if at 300 °C we observe a decelerating pattern characteristic of diffusion control [17], at 360 °C the weight gain is linear (Fig. 3a), i.e. the rate is constant. It means that at 360 °C the rate determining step is a reaction whose progression is not affected by thickness of ZnS layer. We can speculate that the rate determining step is the decomposition of thiophene (hydrodesulfurization) on Ni particles yielding H_2S. This assumption is indirectly confirmed by the fact that activation energy observed for Ni/ZnO for $X > 0.25$ (44 kJ/mol) is close to the value found for Ni/SiO_2 (40 kJ/mol). At temperatures lower than 360 °C the rate of diffusion become comparable to the rate of thiophene hydrodesulfurization and the shape of the conversion profile deviates from the linear one (Fig. 3a). More studies are needed however to confirm this explanation.

Variation of thiophene pressure at 330 °C influences not only the average rates (Table 3) but also the shape of the conversion profiles (Fig. 3b). The average rate increases linearly with thiophene pressure (Fig. 6b) showing that the reaction is of the first order relatively to thiophene.

4. Conclusions

Thiophene reactive adsorption on Ni/SiO_2 and Ni/ZnO proceeds in different ways. In the case of Ni/SiO_2, when only

Ni can be sulfided, the conversion profile has the shape characteristic of heterogeneous reactions controlled by advance of the reaction interface. After a rapid formation of surface sulfide, a slower bulk sulfidation occurs with maximum conversion depending on conditions. The observed conversion profile can be fitted by an exponential equation corresponding to a reaction of first order relatively to Ni and to thiophene. Low value of the activation energy (40 kJ/mol) and a linear pressure dependence of the reaction rate allow to exclude the ionic diffusion as a rate determining step in this case. More generally, we suppose that for reacting nanoparticles it is hardly possible to distinguish chemical steps from diffusion due to very low thickness of the product layer (few Å after 0.5 conversion).

Reaction between Ni/ZnO and thiophene shows a more complex pattern in which at least three different steps can be distinguished. The first one, fast sulfur chemisorption, is followed by a nucleation-controlled sulfidation of ZnO surface. This means that bulk sulfidation of Ni particles does not occur and sulfur species, formed through thiophene decomposition, react preferably with ZnO. After the end of the surface sulfidation (conversion *ca.* 0.25) the reaction rate decreases. The shape of the corresponding part of the conversion profiles varies considerably with temperature. This can be due to the fact that two different processes have comparable rates in this temperature domain and their contributions vary smoothly with temperature due to the difference in activation energies.

Acknowledgement

Financial support from Regional Council of Burgundy (program FABER) is gratefully acknowledged.

References

[1] I.V. Babich, J.A. Moulijn, Fuel 82 (2003) 607.
[2] C. Song, Catal. Today 86 (2003) 211.
[3] E. Ito, J.A. Rob van Veen, Catal. Today 116 (2006) 446.
[4] S. Brunet, D. Mey, G. Perot, C. Bouchy, F. Diehl, Appl. Catal. A Gen. 278 (2005) 143.
[5] G.P. Khare, US Patent 6,274,533 (2001).
[6] K. Tawara, T. Nishimura, H. Iwanami, Sekiyu Gakkaishi 43 (2000) 114.
[7] G. Germana, D. Abbott, U. Turuga, Hydorcarbon Eng. (2004) 35.
[8] P. Burattin, M. Che, C. Louis, J. Phys. Chem. B 104 (2000) 10482.
[9] D.G. Mustard, C.H. Bartholomew, J. Catal. 67 (1981) 186.
[10] C.H. Bartholomew, P.K. Agrawal, J.R. Katzer, Adv. Catal. 31 (1982) 135.
[11] J.A. Rodriguez, J. Hrbek, Acc. Chem. Res. 32 (1999) 719.
[12] A.M. Saib, A. Borgna, J. van de Loosdrecht, P.J. van Berge, J.W. Geus, J.W. Niemantsverdriet, J. Catal. 239 (2006) 326.
[13] T. Schalow, B. Brandt, D.E. Starr, M. Laurin, S. Shaikhutdinov, S. Schauermann, J. Libuda, H.-J. Freund, Angew. Chem. Int. Ed. 45 (2006) 3693.
[14] J. Szekely, J.W. Evans, H.Y. Sohn, Gas-solid Reactions, Academic press, 1976 (Chapter 3).
[15] Z. Grzesik, Solid State Ionics 154–155 (2002) 387.
[16] P. Kofstad, High Temperature Corrosion, Elsevier Applied Science, London, NY, 1988 (Chapter 13).
[17] P. Barret, Cinétique hétérogène, Gauthier-Villars, Paris, 1973 (Chapter 3).
[18] C.H. Bamford, C.F.H. Tipper, Comprehensive Chemical Kinetics, vol. 2, Elsevier, Amsterdam, 1972, p. 71 (Chapter 3).